Journal of Materials Science & Surface Engineering, 6(1): 749-754
ISSN (Online): 2348-8956; 10.jmsse/2348-8956/6-1.4

Dual Growth of Thin Films/Quantum Dot Films by Lab-made Pulsed Laser Deposition for Photonic Devices Application

N. A. Ali[1] . A. Abou Elmagd[2] . Y. Badr[2]

[1]Department of Engineering Physics and Mathematics, Faculty of Engineering, Tanta University.
[2]National Institute of Laser Enhanced Sciences, Cairo University.

ABSTRACT
The presented work describes the use of simple configurations in a lab-build pulsed Laser deposition (PLD) system for the preparation of nano structure thin layers and quantum dots (QDs) films. Excimer laser (308 nm, 8 mj) was utilized to grow semiconductor samples as ZnS thin layers and GeS quantum dots thin films. The structure, optical and morphology of the films were observed by UV-VIS absorption, SEM, and XRD. The results reveal the quantum confinement and the crystalline structure of the prepared films. SEM show that films grown on SiO_2 at 10^{-5} mbar are flat, dense and composed of crystallites of the same stoichiometry as the bulk materials. The AFM images of the QDs thin layers illustrate the creation of homogenous quantum-dots films in the order of 9nm in height. The photoconductivity of the deposited film was also measured. The results indicate an efficient performance of the deposited films as an optical detector.

ARTICLE HISTORY
Received 02-10-2017
Revised 22-11-2017
Accepted 03-12-2017
Published 06-01-2018

KEYWORDS
Thin Films, PLD, semiconductors, SEM, AFM

Introduction

Wide variety of materials have been ablated and deposited as thin films by laser ablation. This fabrication technique obtains a lot of attention lately because of its simplicity. Film growth techniques provides new physical properties in the produced thin films, which would open novel perspectives in many technologies[1-5]thermoelectric, fuel cells, and the energy technology as in the photovoltaic's. Also the applications of thin films are in electronics as semiconductor or devices [6-8]. Pulsed laser deposition (PLD) [9-11,17] is one of the most advanced growth techniques for thin films fabrication[12-13].Different method have been used for deposition of thin films on different substrates such as sputtering [14] , evaporation [15], and chemical vapor deposition (CVD) [16]. PLD is a simple technique that guarantees the needed conditions to grow wide range of materials, since it is possible to change various parameters such as: laser wavelength, pulse duration, ambient gas pressure, energy per pulse, target-substrate distance and substrate temperature to control the size and distribution of particles [18-19].

Wide gap semiconductors thin films have recorded a great progress in the fabrication of solid state laser. To that extent, research efforts had focused on the deposition of films using epitaxial growth of high quality films mainly to improve optical and electrical characteristics of the fabricated devices. ZnS semiconductor material has the largest band gap energy of 3.6 eV at room temperature among the II-VI compound semiconductors. For this reason, it considered one of the most promising materials for optoelectronic devices. GeS is orthorhombic IV-VI semiconducting and gain its importance due to their photoelectric properties, it is radiation sensitive material with very high optical resolution and very good optical properties, which make them usable in optical switching, optical interconnections and optical sensing. GeS film has been suggested to be used successfully as photosensitive film in TV camera tubes.

The low cost, lab-built PLD setup was used to deposit different semiconductors as ZnS crystalline thin layers, and GeS as quantum dots layers. All the prepared samples are studied and characterized by different techniques to validate the features of our homemade system.

Experimental

The PLD method of thin film growth involves evaporation of a solid target in an UHV chamber by laser pulses. The chamber is made in a cylindrical shape of suitable size using steel with six pores. Our pumping system is composed of a rotary pump connected in series with a diffusion pump that can reach maximum pressure of 10^{-6} mbar. The inlet of the diffusion pump is directly attached to the chamber without connecting tubes to eliminate any source of stiffness in the pumping line and to obtain high vacuum efficiency. The features of the ultra-high vacuum (UHV) chamber were outlined elsewhere in [20]. Despite these pumping precautions, pressure could be reduced during operation at high temperatures. However operation at UHV conditions i.e. 10^{-4} – 10^{-10} mbar limits heat loss through radiation only. The evaporating source in our system is an Excimer laser, XeCl, model OPTEX produced by LAMBDA PHYSIK with wavelength 308 nm [21-22]. It operates with repetition rate of (200Hz), maximum pulse energy of (10mj) and pulse duration of 6ns, the short pulse duration enables the laser to retain its high energy. The substrate to target distance is kept at 3cm. Laser beam is guided to the sample through a quartz lens (focal length of 23cm) with incident angle of45°.The substrate temperature is measured by a thermocouple, which is fixed on the substrate holder. The sample is rotated by an Ac induction motor with a simple speed control circuit to give a speed in the range of 4-6 rpm.

In the present work, we produce thin nanolayer using single target material, and QDs layer when using dual target. For single target, the sample (ZnS semiconductor)is fixed at the center of the holder, while rotating 360 degree during the laser irradiation. On the other hand, for

Corresponding Author: N A Ali, Tel: +201116406264
Email: naboulfotoh@zewailcity.edu.eg
Contents lists available at http://www.jmsse.org/ & http://www.jmsse.in/

quantum dots (QDs) preparation using dual sample technique, the target composed of half disks of both samples fixed together on the holder [23] and a stepper motor is used to rotate the target 160° forward and back during the deposition. Figure 1 shows the dual target that was used to grow the GeS QDs embedded in Al2O3 matrix. Prior to the deposition of the GeS QDs, a base layer of alumina was grown on the Quartz substrates. 6-layer of GeS QDs and alumina capping layer was grown by the alternate ablation of the respective targets. The capping layer of alumina and GeS were grown using fixed number of laser pulses equal to 2000 pulses, to grow the QDs of fixed layer thicknesses. In our deposition matrix we kept all parameters fixed to obtain constant fluence of 4.5 J/cm², to investigate the performance of the setup with different target structure. At such short deposition times and intermediate Laser energy, the growth occurred preliminarily in its initial form of isolated islands.

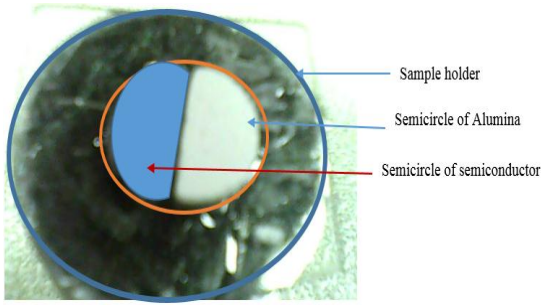

Figure 1: Two target materials fixed on the holder

Semiconductors have been chosen as substrates for epitaxial growth to provide lower lattice mismatch with the target material but in case of optical sensors transparent substrates are preferable as fused silica and quartz. It's known that, films deposited on dirty substrates will frequently cause imperfection or in some cases look uniform but have too low reflectance or transmittance. To avoid these defects, the substrates of suitable dimensions were carefully cleaned as following;

The substrates were washed with hot distilled water and then immersed in dilute NaOH solution for 15 minutes. They were washed several times with distilled water again, and then immersed in chromic acid for 24 hours. Finally they washed with distilled water several times again and with isopropyl alcohol and left to dry in desiccators.

The optical absorption spectra were measured with a dual beam spectrometer SHIMADZU (uv-3101pc- UV-VIS-NIR). The XRD, Philips APD 3720 X-ray diffractometer with Cu K α (λ=1.5406Å) was used to examine the films structure and crystallinity with 2θ scan range from 30 to 75 degree. JEOL 6400 scanning electron microscopy SEM was used to investigate the sample surface morphology in low and high magnifications. SEM was operated at 10-15 keV depending on the conductivity of the sample surface. Further morphological examination and growth of QD thin film was checked bya VEECO Atomic Force Microscope AFM.

One of the requirements of thin film production technology is to provide smooth and uniform film surface. A home-made set up was built for film surface monitoring. As shown in Fig. 2, the beam from a light source incident on a sample through 0.5 mm slit. The sample holder is a moving stage with 0.5 mm step. The transmitted light from the sample is collected by photodiode detector which is connected to digital multi-meter readout device.

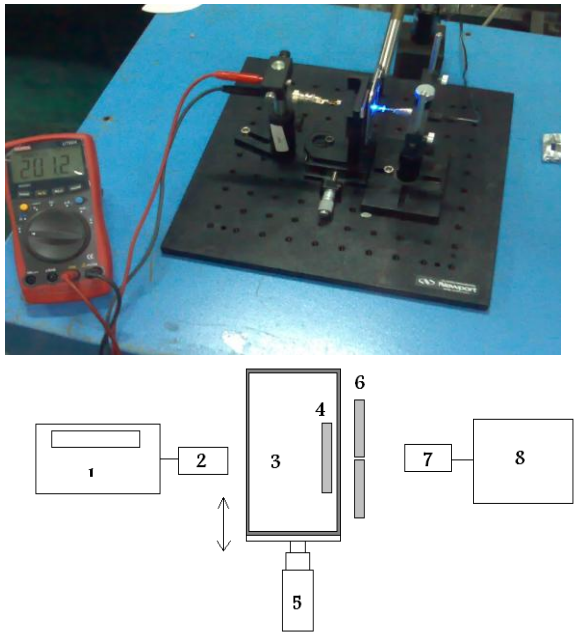

Figure 2: Thickness monitor setup, the schematic diagram of thickness uniformity, 1- Digital Multi-meter, 2- Photodiode, 3- Moving Stage, 4- Sample, 5- Micrometer, 6- Slit, 7- Light Source, 8- Power Supply

The electrical conductivity of some thin films and bulk samples are measured by an electrical circuit. The input voltage is supplied using DC power supply connected in series with the sample; the results are taken as voltage drop on a resistor and then converted into current using the resistance value.

To investigate the performance of the prepared samples to be utilized in the photonic devices, the photoconduction was measured. The used experimental setup consists of a diode laser in spectral line of 808 nm with the availability to change the input power of the laser and then the intensity of the incident beam. A digital electrometer (is connected in parallel with a resistor), and a programmable DC voltage source were employed to bias the sample as shown in Fig. 3.

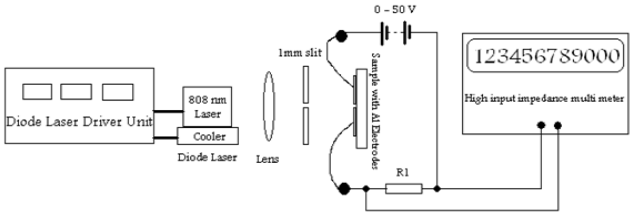

Figure 3: Schematic diagram of Photoconduction setup

The contacts were made of Aluminum prepared by thermal evaporation on the film surface as shown in Fig. 4. Therefore the electrical field is applied along a gap of 1mm between the Al contacts clearly exceeds the film thickness, then the applied electric field was dispersed uniformly through the sample.

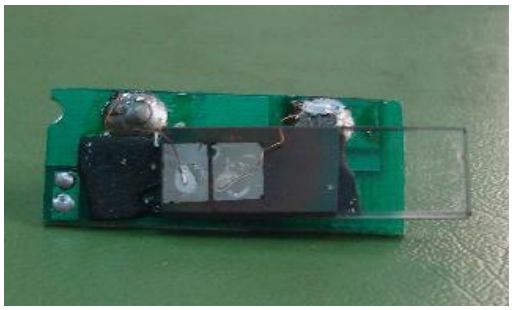

Figure 4: Al electrodes on the thin film sample.

Results and Discussion

Using 308 nm Excimer, with energy 5mJ/pulse to incident on pure ZnS target and focused to 5μ yields a fluence of 10^4 J/cm^2. The produced thin films were subjected to optical analysis including, absorption in the UV/VIS region and fluorescence after being excited at 260 nm as Compared to bulk target materials. Figure 5 (a) shows the absorption spectra of the bulk ZnS and the deposited film. The optical absorption spectrum of both samples consists of wide range of wavelengths mostly in the UV range. The absorption peaks of the film are obviously shifted toward the blue region. Figure 5 (b) represents the fluorescence spectra of the ZnS bulk and deposited film, after excitation by 260nm. The fluorescence of the film is shifted also to the blue region of the spectrum which confirms the confinement effect in one direction. Intensities of absorption and fluorescence are much higher in bulk sample than in thin film, which indicates that absorption of photons is higher in bulk material than thin films.

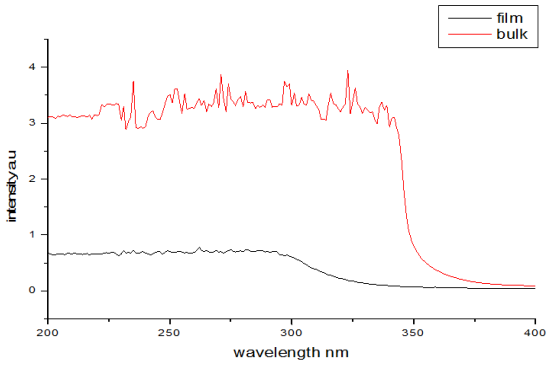

(a)

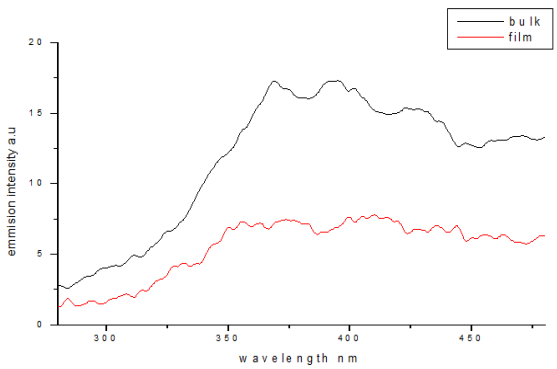

(b)

Figure 5: (a) Optical absorption of ZnS bulk and deposited film, (b) The fluorescence spectra of ZnS bulk and deposited film samples

As illustrated in the experimental setup of the film uniformity, its goal is to show the morphology of the film surface presented in x-y curves, where the X-axis represents the distance over the film surface starting at one edge passing through the other edge. While Y-axis represents the transmittance intensity. Figure 6 illustrates the transmittance from (a) ZnS and (b) GeS thin films over the liner distance. The results illustrate that the lab-made deposition system succeeded to produce uniform thin layers over linear range of 10 mm.

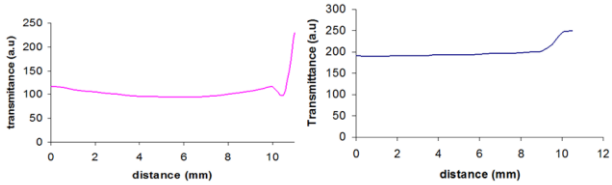

(a) (b)

Figure 6: Transmittance spectrum of (a) ZnS thin film, (b) GeS thin film to show the uniformity over the surface

EDX is a technique used for identifying the elemental composition of the sample. As shown in the EDX results represented in Fig. 7 (a) for ZnS bulk target that confirm the percentage of its essential elemental components in comparison to the amount of trace elements that are negligible, while Fig. 7(b) shows the DEX results of elemental composition of the ZnS thin film which are Zn And S and some impurities as Al and Cl. The great percentage of Si and Oxygen is due to the composition of the quartz substrate.

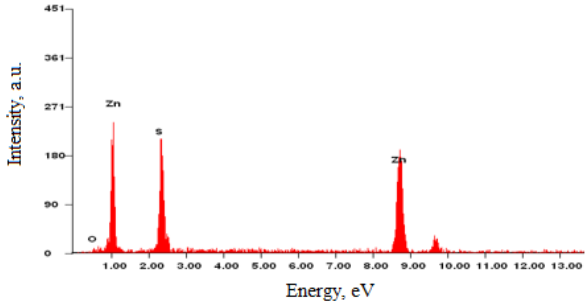

(a)

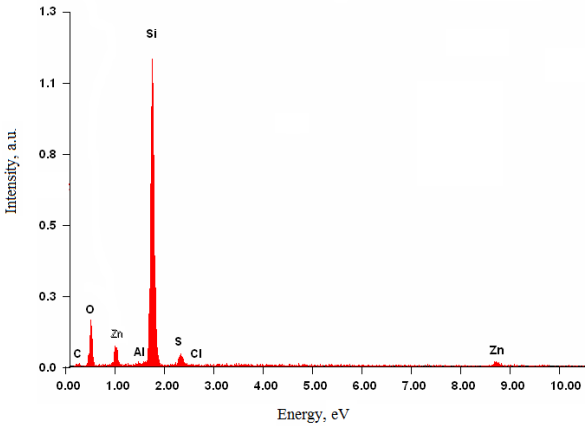

(b)

Figure 7: The EDX results of (a) ZnS bulk material, (b) ZnS thin film on quartz

Figure 8 shows the X- Ray diffraction pattern for GeS and ZnS samples. For ZnS thin film, the diffraction peaks can be indexed to the planes (111), (200), (220), (331) of the cubic crystal phase of ZnS. In Fig. 8(b) the diffraction pattern of GeS film indexed to the plans (210), (111), (400), (311), (002) referring to the orthorhombic structure of GeS. It is interesting to note that the diffraction pattern exhibit good similarity to crystal structure of bulk ZnS and GeS [24], suggesting that growth by the lab-build PLD keep the stoichiometry of the target material in the deposited thin layer. The lattice parameters of the cubic structure are equal to $a = b = c = 5.4$ Å. The particle size was calculated using Scherrer's formula [25].

$$D = k\lambda/\beta \cos\theta \qquad (1)$$

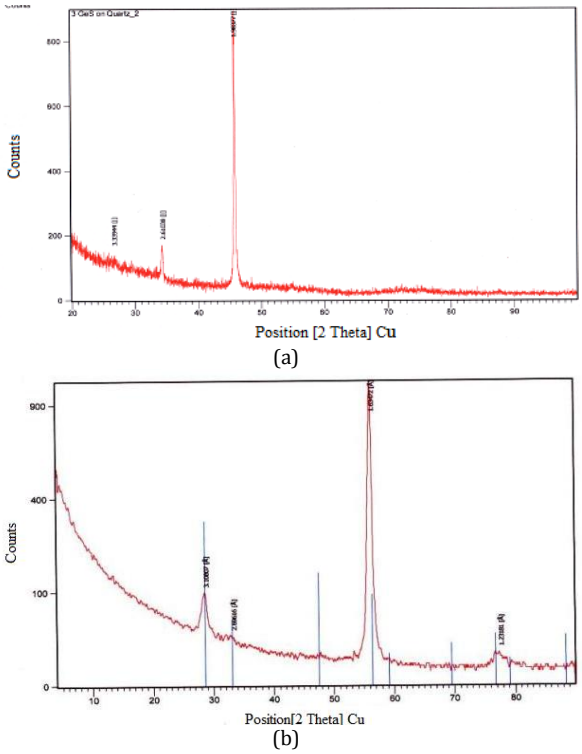

Figure 8: XRD results of (a) GeS thin layer on quartz substrate, (b) ZnS thin layer on quartz substrate.

Where D is the crystallite thickness measured perpendicular to the reflecting plane, k is the Scherrer's constant the value of which is chosen as 0.9 by assuming the particle to be spherical, λ is the wavelength of X-ray radiation, β is the width at half the maximum intensity measured in radians and θ is the Bragg angle. Four θ values corresponding to the most significant intensities planes are selected. The average crystallite size is 13 Å for GeS and 16 Å for ZnS thin films.

The Scanning Electron Microscope SEM images are shown in Fig. 9 (a) for ZnS bulk sample, and Fig. 9 (b) for GeS bulk target material, Fig. 9 (c) ZnS thin film deposited on quartz. While Fig. 9 (d) indicates the ZnS deposited film fused silica.

Images of ZnS and GeS target materials showed dense crystalline structure, and the images of produced thin films showed homogeneous morphology without any distinguishable particulates on the entire film surface. This confirms the conveniences of the lab setup to produce smooth and homogeneous films. The morphology of the deposited film on the crystalline substrate appears smoother and without any pores or defects than the ZnS film that deposited on amorphous substrate, which reflects the effect of the substrate crystallinity.

The AFM was used to study the growth of GeS QDs on Quartz substrate. Germanium sulfide is the target while Al_2O_3 is the capping material. It was targeted to achieve the growth of GeS on Quartz substrate in the desired size of the QDs before the onset of coalescence of islands and formation of a continuous layer.

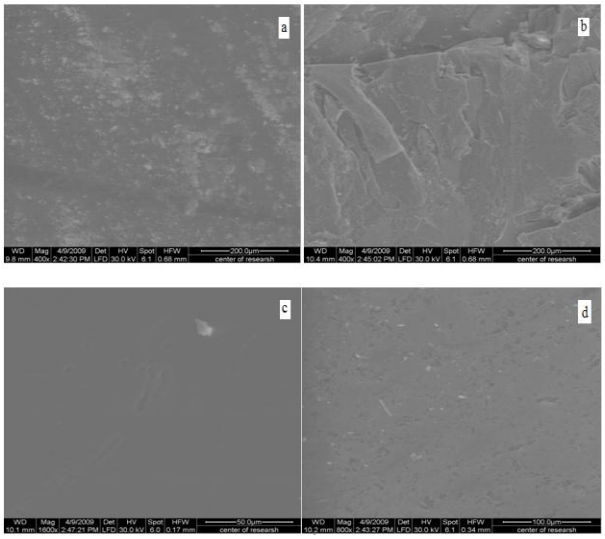

Figure 9: SEM images of (a) Bulk ZnS Semiconductor target, (b) Bulk GeS Semiconductor target, (c) ZnS film on quartz substrate, (d) ZnS film on fused silica

Figure 10(a) shows an AFM image of a typical area of GeS quantum dots by our PLD setup, while Fig. 10(b) shows the 3D image of the same sample. It is clear that the dimension of the single quantum dots is in nm scale and Root mean square roughness over an area of 0.8μm x 0.8μm was < 1 nm, which implies that the film is homogeneous and without cracks. Results also show islands with different sizes. Most of the islands are dome shaped with well-defined facets. Scans of islands, taken along their major axes are shown. The facets were identified by the angle they make with crystalline plane. The average height of the dots is ~ 17 nm and islands density is $\sim 1.5\times10^{9}$ cm^{-2}.The dimension of the single quantum dot is base diameter about 150 nm and height about 9.0 nm as shown in Fig. 10 (c), This result indicates that the height of the dot can be well controlled by deposit more or less layers.

The conductivity was measured at different temperatures beginning from room temperature through higher values as shown in Fig. 11(a) for bulk, (b) for thin film, where conductivity is presented as current response on Y-axis verses the input voltage on X-axis, at three values of temperatures, namely: 19◦C, 50◦C and 75◦C. The results show linear relation between the input voltage and the current response but there is no significant effect of increasing the temperature. Which guarantee very good operation for such material even with elevated temperature. The film samples show much higher values of resistance than the bulk.

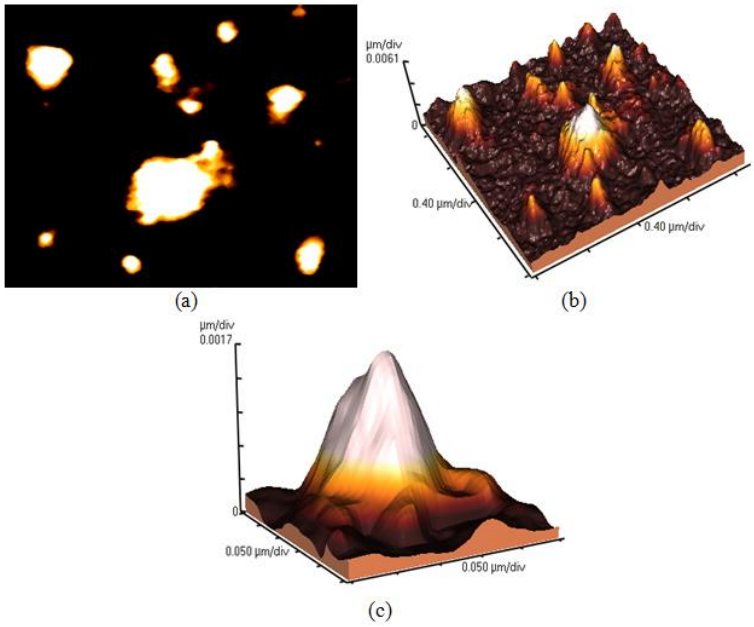

Figure 10: AFM image for GeS quantum dot (a) 2D image, (b) 3D image, and (c) single quantum dot

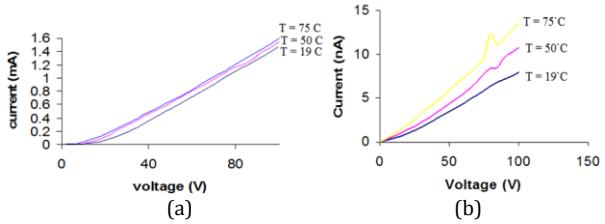

Figure 11: Current vs. voltage plots of GeS, (a) bulk sample with different temperatures, (b) thin film with different temperatures

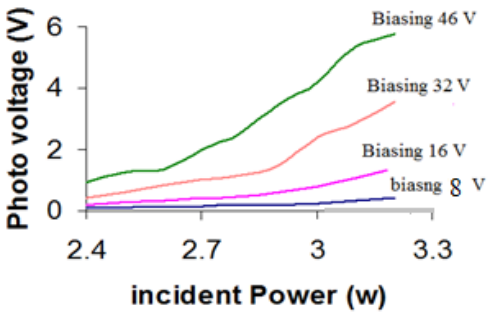

Figure 12: Photoconduction spectra at room temperature of GeS thin film, with different biasing voltage

The optical sensitivity characterization for GeS bulk and thin film is shown in Fig. 12. As shown in the figure the output voltage increases linearly with the incident powers of 808 nm laser diode at different values of the applied bias. In addition the linearity of the curves increase by increasing the biasing voltage from 8 volt to 46 volt which indicate the better expected photo response [26-30] behavior of the film as an optical detector in the NIR range at higher values of bias voltage.

Conclusions

Pulsed laser deposition lab-build system was used in the preparation of quantum dots GeS layers on quartz substrate. Films with different thicknesses were produced by varying the number of pulses. Homogeneous surface morphology of has been proven for the deposited films by SEM, and XRD analysis confirms the crystal structure of the films. AFM results illustrate the formation of almost uniform quantum dots of average height 9 nm. The photoconductivity of the films shows a linear response to the NIR photons. Better response is observed at higher bias voltages.

The significance of the results is that the low cost PLD system that was built in our lab can produce thin layers in different structure as nano-layers and quantum dot thin films. Moreover, the chosen low cost semiconductor material was used to produce thin layers that achieve very efficient performance as optical detectors, or photocells.

References

1. V. A. Egorov, G. É. Cirlin, A. A. Tonkikh,V. G. Talalaev, A. G. Makarov, N. N.Ledentosov, V. M. Ustinov, N. D. Zakharov, P. Werner, Si/Ge nanostructures for optoelectronics applications, Phys. Solid State, 2004, 46(1), 49-55.
2. A. Elfving, G. V. Hansson, and W.-X. Ni,SiGe (Ge-dot) heterojunction phototransistors for efficient light detection at 1.3–1.55µm, Physica E., 2003, 16 528-532.
3. J. L. Liu, A. Khitun, K. L. Wang, T. Borca-Tasciuc, W. L. Liu, G. Chen, D. P. Yu, Growth of Ge quantum dot superlattices for thermoelectric applications, J. Cryst. Growth,2001, 227-228, 1111-1115.
4. A. Alguno, N. Usami, T. Ujihara, K.Fujiwara, G. Sazaki, K. Nakajima, Y.Shiraki, Super-dense array of Ge quantum dots grown on Si(100) by low-temperature molecular beam epitaxy, Appl. Phys.Lett.,2003, 83,1258-1260.
5. V. Ryzhii,The theory of quantum-dot infrared phototransistors,Semicond. Sci.Technol. , 1996, 11 759-765.
6. M. Maksimović, Quantum Dot Infrared Photodetector as an Element for Free-Space Optics Communication Systems , XI TELEKOMUNIKACIONI FORUM TELFOR, Nov. 2003 Beograd, Sava Centar.
7. M. S. Hegazy , Tamer F. Refaat T, and H. E. Elsayed-Ali, Self Assembled Quantum Dot Mid-infrared Si/Ge Photodetector Fabricated by Pulsed Laser Deposition, 6th WSEAS International Conference on CIRCUITS, SYSTEMS,

ELECTRONICS,CONTROL & SIGNAL PROCESSING, Dec. 2007, Egypt,.
8. H. C. Liu, "Quantum dot infrared photodetectors," Optoelectronics Rev., 2003, 11(1), pp. 1-5.
9. M. S. Hegazy , H. E. Elsayed-Ali, Self-Assembly of Ge Quantum Dots on Si(100)- 2×1 by Pulsed Laser Deposition, Appl. Phys. Lett. 86 (2005) 243204.
10. M. S. Hegazy and H. E. Elsayed-Ali, Growth of Ge quantum dots on Si by pulsed laser deposition, J. Appl. Phys. 99, 2006, 054308.
11. T. F. Refaat, M. N. Abedin, O. V. Sulima, U. N. Singh and S. Ismail, IEDM Technical Digest. IEEE International Electron Devices Meeting, Dec. 2004, 355-358.
12. V. Cimalla, K. Zekentes, and N. Vouroutzis, "Control of morphological transitions during heteroepitaxial island growth by reflection high-energy electron diffraction," Mater. Sci. Eng. B 88,2002, pp. 186-190 (2002).
13. P. S. Chen, Z. Pei, Y. H. Peng, S. W. Lee, M.-J Tsai, "Boron mediation on the growth of Ge quantum dots on Si (100) by ultra high vacuum chemical vapor deposition system," Mat. Sci. Eng. B 108, 2004, pp. 213-218.
14. Martin A. Noah1,a), Zumin Wang1,2, and Eric J. Mittemeijer, Interdiffusion in amorphous AlxZr1-x alloys, Journal of Applied Physics, 2017, 121, 015302.
15. W.M. Kim, D. Y. Ku, K.S. Lee, B. Cheong ,Effect of oxygen content and deposition temperature on the characteristics of thin silver films deposited by magnetron sputtering, Applied Surface Science,2010, 257 (4).
16. T.Petkova,V.Ilcheva,P. Petkov, G. Socol, C. Ristoscu, F. Sima, C . N. Mihailescu, I. N. Mihailescu, C. Popov, V. Boev, J.P. Reith maier, "Stress study of thin AsSeAg films obtained by vacuum thermal evaporation and pulsed laser deposition", Journal of Optoelectronic and Advanced Materials,2010, 12 (3), 650653.
17. Mehdi Ranjbar, Parviz Kameli, Hadi Salamati, Coalescence threshold temperature in Ag nano-island growth by Pulsed laser deposition, Materials Physics and Mechanics,2013, 17, 22-28
18. J.C. Alonso, R. Diamant, P. Castillo, M.C. Acosta-García, N. Batina, E. HaroPoniatowski ,Thin films of silver nanoparticles deposited in vacuum by pulsed laser ablation using a YAG:Nd laser, Applied Surface Science,2009, 255 (9), 4933.
19. Yang F. L., Somekh R. E., Greer A. L. UHV magnetron sputtering of Ag films on rocksalt: quantitative X-ray texture analysis of substrate-temperature-dependent microstructure. Thin Solid Films, 1998, 322(1–2), 46–55
20. N.A. boulfotoh, A. AbouElmagd, M. Atta, B.Moharam,Y. badr, Design andperformance of optical detectors fabrication setup using pulsed lased deposition (PLD), The 7th International Conference of Laser Application-ICLA, May 2009, AIP. 978-0-7354-0711.
21. S. M Green, A. Pique, K. S. Harshavardhan , J. Bernstein, Pulsed Laser Deposition of thin films, in: Douglas B Chrisey and Graham K. Hubler (Eds), 1998, John Wiley & Sons, Inc., New York.
22. Lambada Physik, OPTex Eximer Laser User manual, LP Part No. 263 292, (1999).
23. H. Zabel and S. D. Bader (Eds.), Magnetic Heterostructures, Landolt–Bornstein Handbook [New Series 111/14b2], Springer, Berlin Heidelberg, 2008.
24. G K Solanki1, Dipika B Patel, Sandip Unadkat, M K Agarwal, Synthesis and characterization of germanium monosulphide (GeS) single crystals grown using different transporting agents , PRAMANA - journal of physics, 2010, 74- 5,813-825.
25. B D Cullity, Elements of X-ray diffraction, 1978, Addison-Wesley, 2nd edition, p. 102.
26. D.M.M. Atwa, I. M. Azzouz, Y. Badr , Optical, structural and optoelectronic properties of pulsed laser deposition PbS thin film,Appl. Phys. B, 2011, Volume 103, Issue 1, pp 161–164
27. Qilin Dai, Erwin M. Sabio, Wenyong Wang, and Jinke Tang, Pulsed laser deposition of Mn doped CdSe quantum dots for improved solar cell performance Appl. Phys. Lett. 104, 183901 (2014)
28. Qilin Dai, Jiajun Chen, Liyou Lu, Jinke Tang, and Wenyong Wang, PbS quantum dots prepared by pulsed laser deposition for photovoltaic applications and ligand effects on device performance, Appl. Phys. Lett., 2013, 102, 203904.
29. Ibrahima Ka, Vincent Le Borgne, Kazunori Fujisawa, Takuya Hayashi, Yoong Ahm Kim, Morinobu Endo, Dongling Ma & My Ali El Khakani, Multiple exciton generation induced enhancement of the photo-response of pulsed-laser-ablation synthesized single-wall-carbon-nanotube/PbS-quantum-dots nanohybrids, Scientific Reports 6, 2016, Article number: 20083.
30. I. Ka, B. Gonfa, V. Le Borgne, D. Ma, M. A, Pulsed Laser Ablation Based Synthesis of PbS-Quantum Dots-Decorated One-Dimensional Nanostructures and Their Direct Integration into Highly Efficient Nanohybrid Heterojunction-Based Solar Cells, Adv. Funct. Mater. 2014, 24, 4042–4050.